


RESEARCH ARTICLE

Evaluation of pathogenesis and biofilm formation ability of *Yersinia pestis* after 40-day exposure to simulated microgravity

Ye Li , Yulu Chen, Lei Wang, Yixuan Li, Yajun Song, Ruifu Yang and Yanping Han

State Key Laboratory of Pathogen and Biosecurity, Beijing Institute of Microbiology and Epidemiology, Beijing, 100071, China

Author for correspondence: Yanping Han, E-mail: hypiota@hotmail.com

Received: 07 July 2021; **Accepted:** 24 January 2022; **First published online:** 28 February 2022

Key words: Biofilm, cytotoxicity, simulated microgravity, virulence, *Yersinia pestis*

Abstract

With the increase of crewed space missions and the rise of space microbiology, the research of microbes grown under microgravity environment has been attracting more attention. The research scope in space microbiology has been extended beyond pathogens directly related to spaceflight. *Y. pestis*, the causative agent of plague, is also of interest to researchers. After being cultivated for 40 consecutive passages in either simulated microgravity (SMG) or normal gravity (NG) conditions, the *Y. pestis* strain 201 cultures were analysed regarding their phenotypic features. By using crystal violet staining assays, increased biofilm amount was detected in *Y. pestis* grown under SMG condition. Besides that, the damage degrees of HeLa cell caused by SMG-grown *Y. pestis* were found diminished in comparison to those under NG condition. Consistent with this observation, the death course was delayed in mice infected with SMG-grown *Y. pestis*, suggesting that microgravity condition can contribute the attenuated virulence. RNA-seq-based transcriptomics analysis showed that a total of 218 genes were differentially regulated, of which 91 upregulated and 127 downregulated. We found that dozens of virulence-associated genes were downregulated, which partially explained the reduced virulence of *Y. pestis* under SMG condition. Our study demonstrated that long-term exposure to SMG influences the pathogenesis and biofilm formation ability of *Y. pestis*, which provides a novel avenue to study the mechanism of physiology and virulence of this pathogen. Microgravity enhanced the ability of biofilm formation and reduced the virulence and cytotoxicity of *Y. pestis*. Many virulence-associated genes of *Y. pestis* were differentially regulated in response to the stimulated microgravity. However, there is no molecular evidence to explain the enhanced biofilm formation ability, which requires further research. Taken together, the phenotype changes of *Y. pestis* under SMG conditions can provide us a new research direction of its potential pathogenesis.

Contents

Introduction	97
Material and method	97
Bacterial Strains and culture conditions	97
Crystal violet staining	98
RAW 264.7 cells intracellular survival assay	98
HeLa Cells cytotoxicity/rounding assay	98
BALB/c mice infection assay	99
RNA-seq-based Transcriptional analysis	99
Quantitative real-time PCR	99
Results	99
Assessment of biofilm formation ability of <i>Y. pestis</i> grown under SMG	99
Assessment RAW 264.7 cells intracellular survival ability of <i>Y. pestis</i> grown under SMG	100
Assessment of cytotoxicity of <i>Y. pestis</i> under SMG	100

Assessment of virulence of <i>Y. pestis</i> under SMG	101
Detection of the differential expressions of 218 genes between SMG and NG groups.	102
Discussion	104
Conclusions	107
Authors contributions	108

Introduction

Long-term exposure to the outer space environment may have blunted the immune functions of astronauts, which can increase the risk of infectious diseases caused by certain pathogenic microbes (Sonnenfeld and Shearer, 2002; Buchheim *et al.*, 2019). Microgravity is a key factor of the outer space environment, where microbes can adapt and respond to the special environment stress through gene modification and phenotypic alterations (Wilson *et al.*, 2007). Due to expensive cost and limited space, high-aspect-ratio rotating-wall vessels (HARVs) developed by NASA has been applied to cultivate microbes and thus provide low-shear simulated microgravity (LSSMG) in the conventional laboratory (Nickerson *et al.*, 2004; Rosenzweig *et al.*, 2010; Wang *et al.*, 2016). *Salmonella typhimurium* showed increased virulence and resistance to acid stress and macrophage killing under SMG (Nickerson *et al.*, 2000; Wilson *et al.*, 2002b), on the contrary, diminished virulence was found in some bacteria grown under SMG (Castro *et al.*, 2011).

The genus *Yersinia*, a member of the family *Enterobacteriaceae*, is composed of 11 species, three of which (*Y. pestis*, *Y. pseudotuberculosis*, and *Y. enterocolitica*) are pathogenic for rodents and humans (Perry and Fetherston, 1997). The most notorious species, *Y. pestis*, is the causative agent of plague. After *Y. pestis* invades the host, the type III secretion system encoded by the pCD1 plasmid can secrete a variety of effector proteins, which can inhibit the phagocytosis of host macrophages and down-regulate the inflammatory response, so that the *Y. pestis* can survive and multiply in the host (Pujol and Bliska, 2005). The deadly pathogen is always maintained in nature dependent upon cyclic transmission between fleas and mammals. *Y. pestis* is regarded as a model pathogen for studying the mechanism of vector-mediated dissemination and pathogenesis.

Surprisingly, two non-pathogenic members of *Yersinia* genus, *Y. frederiksenii* and *Y. intermedia* have been found during several spaceflights of the International Space Station (Singh *et al.*, 2018). Low-shear force might be common stress upon exposure of *Y. pestis* to spaceflight board or systematic infection within the human body and flea proventriculus. Previously, the Rosenzweig's group has initiated studies on the effect of microgravity on *Y. pestis* growth physiology and virulence potential. *Y. pestis* exhibited the impaired ability of cytotoxicity but no alterations in growth kinetics, cold-resistance, or antibiotic-sensitivity (Lawal *et al.*, 2010, 2013). Blood meals of fleas might provide the low-shear-force-like microenvironment to *Y. pestis*. The blocked bacterial masses in the flea proventriculus due to biofilm formation further contribute to the subsequent spread of mammalian infection. However, biofilm formation ability could not be observed in *Y. pestis* KIM derivative strain lacking of the pigmentation locus *pgm* (Lawal *et al.*, 2013). How *Y. pestis* respond to mid-long-term microgravity stress remains to be investigated. Based on these considerations, here we used the *Y. pestis* biovar *Microtus strain 201*, which is avirulent to humans but highly lethal to mice, to evaluate the strain-specific effects of stimulated microgravity lasting for 40 days on virulence and biofilm production.

Material and method

Bacterial Strains and culture conditions

Y. pestis biovar *Microtus strain 201* was isolated from *Microtus brandti* and is extremely lethal to mice but avirulent to humans and other large animals (Song *et al.*, 2004). *Y. pestis* wild-type (WT) strain 201 was reserved in our lab, and used in this study. In general, *Y. pestis* was grown in lysogeny broth (LB) or agar plate at 26 or 37°C, unless otherwise specified. Resuscitated *Y. pestis* biovar *Microtus strain 201* was inoculated at a dilution of 1:20 into the HARV bioreactors. When HARVs were filled with ~58 ml

fresh LB medium and the bubbles were removed, the simulated microgravity (SMG) condition was generated by the HARVs' axis of rotation perpendicular to the gravity direction. On the contrary, the normal gravity (NG) cultivation condition was generated by the axis parallel to the gravity direction (Wang *et al.*, 2016). There was a silicified gas-permeable membrane on the back of the HARVs, which can provide oxygen supply and prevent the leakage of liquid during bacterial culture.

Under the condition of 26°C and rotary speed of 25 rpm, *Y. pestis* was respectively grown to the middle exponential phase (2×10^8 CFU ml⁻¹) under the SMG and NG conditions, then diluted 20 times to new HARV bioreactors for 40 consecutive passages of cultivation.

Crystal violet staining

The biofilm formation ability of *Y. pestis* is assessed by the crystal violet staining as follows. With the cultures being removed, the bioreactors were washed lightly with phosphate buffer saline (PBS) and then were stained with 0.1% crystal violet solution for 20 min at room temperature.

In order to quantitatively analyse the difference of biofilm formation ability between SMG and NG group, the cultures were taken on a 24-well plate at a dilution of 1:100 (added 10 μ l of bacterial culture to 1 ml of LB per well) and incubated for 24 h on a shaker at 37°C and 200 rpm. The optical density (OD) values were measured for each well at 620 nm. Remove the bacterial solutions thoroughly and put the 24-well plate at 80°C for 15 min to fix the biofilm. Each well was dyed with 3 ml 0.1% crystal violet solution for 15 min and washed three times with PBS. Each well was added with 2 ml dimethyl sulfoxide solution to dissolve the crystal violet, and measured the OD values at 570 nm. Finally, the ratios of OD_{570nm} to OD_{620nm} of each well were calculated.

RAW 264.7 cells intracellular survival assay

We used RAW 264.7 cells to evaluate the bacterial intracellular survival ability. The cultures grown to the middle exponential phase under SMG and NG groups were added to 24-well plates that contained 70–80% single-layer adherent RAW 264.7 cells at a multiplicity of infection (MOI) of ~5. At 0.5 h past infection (hpi), gentamycin was added to kill the extracellular bacteria and the infected cells were lysed by 500 μ l of Triton-X solution. Then living bacteria counting of the lysate was performed on the agar plates in triplicate. The above operations were repeated at 4, 6, 8 hpi.

HeLa Cells cytotoxicity/rounding assay

HeLa cells were selected to evaluate the cytotoxicity of *Y. pestis*. Following the published methods for the HeLa cell rounding/cytotoxicity assay (Lawal *et al.*, 2010), saturated cultures of the SMG and NG groups were added to infect the HeLa cells in 12-well plates for 2.5 h at a MOI of ~50. The HeLa cells cytotoxic effects were evaluated by observing the cell rounding phenotype through optical microscopy.

However, HeLa cells may be rounded due to crowded growth and errors deriving from observing cell morphological changes with naked eyes. We decided to utilize the xCELLigence real-time cell analysis (RTCA, ACEA Biosciences Inc) system to analyse the dynamic and quantitative response profile of HeLa cells *in vitro*, and this technology is non-invasive and label-free. Cellular changes including cell number (cell index, CI) were recorded and analysed via the RTCA system (Pan *et al.*, 2013; Roshan Moniri *et al.*, 2015; Cetin and Topcul, 2019). The principle of the RTCA system is to read the electronic readings change from the gold-plated sensor electrodes located on the bottom of microplates (E-plate). Electronic readings changes as the HeLa cells adhere or detach to the surface of the electrodes, CI values are drawn via the software calculation (Qiao *et al.*, 2008).

HeLa cells were added into the 8-well microplates (E-plate) and cultured at 37°C with 5% CO₂ for 12 h. The bacteria grown under SMG and NG conditions were added into the E-plate for 24 h at a MOI of ~5. The cell index data were collected and analysed by the RTCA Data Analysis Software 1.0, and then the data was reanalysed per 2 h from 3-h to 36-h point using GraphPad Prism 5.0 software.

BALB/c mice infection assay

Saturated cultures grown under SMG and NG conditions were centrifuged at the rotary speed of 4,500 rpm, the supernatant was discarded, and the cells were diluted to a concentration of one hundred microliters containing 100 CFU or 10 CFU with phosphate-buffered saline (PBS). The actual number of bacteria contained per 100 microliters is counted through dropping on the Hottinger's Agar plates. We randomly divided 32 8-week-old BALB/c female mice into four groups, and the diluted bacteria of 40th passage were inoculated into each group with an intraperitoneal route. The infected mice were monitored for 14 consecutive days and recorded the number of dead mice daily. The survival curves were drawn with GraphPad Prism 5.0 software, and the *p*-values less than 0.05 were considered statistically significant through log-rank (Mantel-Cox) test. The BALB/c mice used in this experiment were provided by Beijing Vital River Laboratory Animal Technology Co. Ltd [laboratory animal permit no. SCXK (Jing) 2016-0006]. All mice participating in this experiment were treated in accordance with the guidelines for the welfare and ethics of laboratory animals.

RNA-seq-based Transcriptional analysis

The cultures in SMG and NG bioreactors were grown to saturation ($OD_{620nm} = 1.0$) as mentioned before. Each group was set as three biological replicates. The mRNAs were obtained by removing the ribosomal RNA (rRNA) from the total RNA extracted by the PureLink™ RNA Mini Kit (Invitrogen, Thermo Fisher Scientific, USA), and then used for creating cDNA library and deep sequencing. According to the values of FPKM (Fragments Per Kilobase Million), the ratio of transcript levels between SMG and NG groups were used as the logarithm to the base of 2 (Two-Fold Change), for example, a two-fold change value of 1.0 indicates a 2-fold greater expression of a certain gene. The differential values at least 2-fold were applied to analyse the differential expression of genes according to the *Y. pestis* 91001 genome annotation.

Quantitative real-time PCR

The total RNA was extracted as described above, and purified by TURBO DNA-free™ Kit (Invitrogen, Thermo Fisher Scientific, USA) upon the manufacturer's instructions. The total RNAs were reverse transcribed into cDNA as templates by SuperScript™ Reverse Transcription Kit (Invitrogen, Thermo Fisher Scientific, USA). Seven genes were selected and performed for quantitative RT-PCR (qPCR). All primer pairs were designed to produce amplicons with expected sizes of 50–200 nt through the Primer Premier 5.0 software (Table 1).

Meanwhile, the highly expressed 16S ribosomal RNA gene was chosen as the reference gene to draw the relative standard curve, in order to quantitatively compare and analyse differential expression levels of the target genes. We diluted each cDNA sample to a concentration of $5 \text{ ng } \mu\text{l}^{-1}$ as the template of the qRT-PCR reaction. The components of the qRT-PCR reaction system are shown in Table 2.

The qPCR was carried out in the Light Cycler R480 quantitative PCR instrument (Roche, CA, USA) and its software would calculate the relative fold change of target genes in the RNA samples of SMG and NG groups. The reaction procedure of qPCR is shown as Table 3.

Results

Assessment of biofilm formation ability of *Y. pestis* grown under SMG

The biofilm formation ability was assessed by evaluating the amount of biofilm formed and adhered on the silicified gas-permeable membrane on the back of the bioreactors. We found that the amount of biofilm in the SMG bioreactor was higher than that in the NG bioreactor (Fig. 1(a)).

In order to quantitatively evaluate the biofilm formation ability, the OD_{570nm} values of crystal violet staining were divided by the OD_{620nm} values of cultures in the 24-well plates before staining.

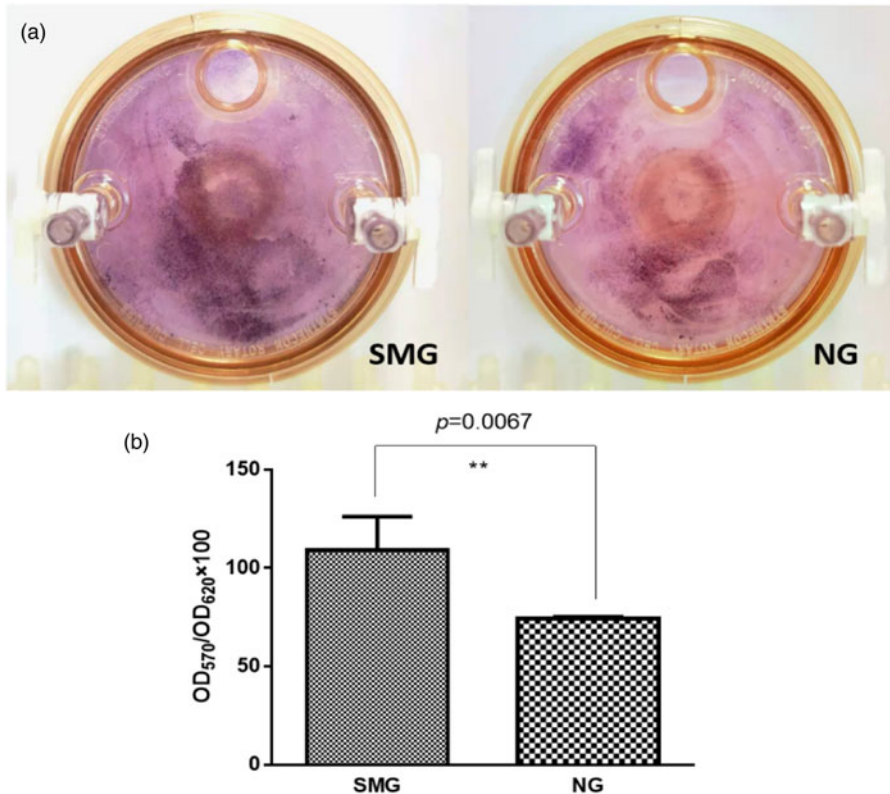


Figure 1. Biofilm measurement of *Y. pestis* grown under SMG or NG conditions by crystal violet staining. (a) The biofilms formed on the back of bioreactors were stained with crystal violet. (b) By calculating the ratio of the OD_{570nm} to OD_{620nm} values, the biofilm formation ability was quantitatively analysed by GraphPad Prism 5.0 software ($p = 0.0067$, using Student *t* test).

This operation eliminated the influence of the different numbers of bacterial in each well. By calculating the ratio of OD_{570nm} to OD_{620nm} values, the SMG group had higher values than the NG group (~109 and 74.3 of mean value in the SMG and NG group, respectively) (Fig. 1(b), $p < 0.05$, using Student *t* test), indicating that SMG condition increased the biofilm formation ability of *Y. pestis*.

Assessment RAW 264.7 cells intracellular survival ability of *Y. pestis* grown under SMG

In RAW 264.7 cells intracellular survival assay, the trend of the SMG group was almost consistent with the NG group (Fig. 2(a)). The mean values of survival rate at 8-hour past infection (hpi) were 2.85% (SMG) and 2.47% (NG), respectively. The survival rates of *Y. pestis* in RAW 264.7 cells at 8-hpi had no statistically significant difference ($p = 0.5835$, using the Student *t* test) between SMG and NG groups (Fig. 2(b)). The figure of 8-hpi was just the representative result in that the same trend was shown at other time points. This result indicated that the microgravity environment cannot change the viability of *Y. pestis* in macrophages.

Assessment of cytotoxicity of *Y. pestis* under SMG

The normal morphology of HeLa cells was irregular fusiform, while the infected HeLa cells were shown varying degrees of rounding. At a MOI of ~50, approximately 23% of SMG-grown *Y. pestis*-infected HeLa cells (Fig. 3(a)) were extremely rounded relative to 68% of NG-grown counterpart

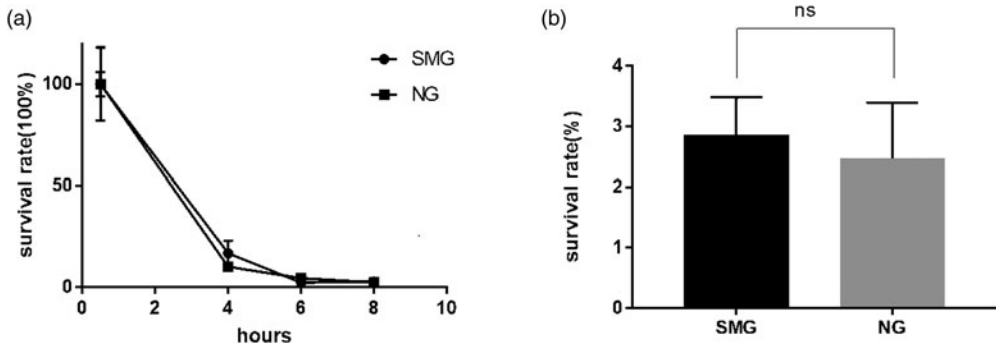


Figure 2. Survival dynamics of SMG- and NG-grown *Y. pestis* within RAW 264.7 macrophages. (a) The amount of RAW264.7 cells in each hole of the 24-well plate is 4×10^4 and RAW 264.7 cells of each hole were infected by $10 \mu\text{l}$ cultures ($OD_{620\text{nm}} = 1$) grown under SMG or NG condition at a MOI of ~ 5 . The survival percentage was expressed as the ratio of the amount of intracellular living bacteria at a certain-time point to the absolute amount of that at 30-min. (b) At 8-hpi, the differences in RAW 264.7 cells intracellular survival rate were not statistically significant.

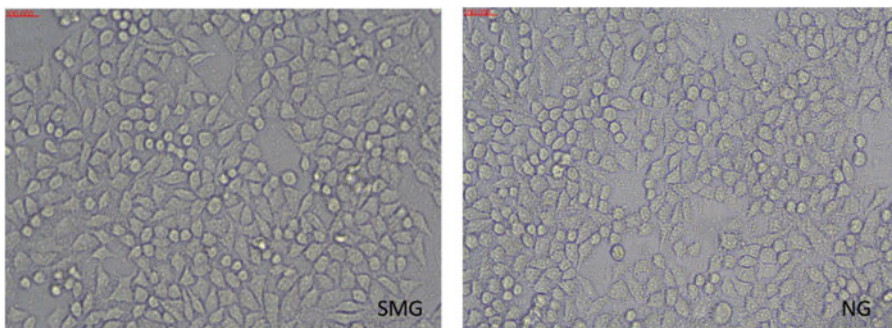


Figure 3. Monitoring of HeLa cells damages by comparing the proportion of rounding cells between SMG and NG group. The saturated HeLa cells were infected by *Y. pestis* grown under SMG (a) and NG (b) conditions at a MOI of ~ 50 , that is, each hole of a 12-well plate contains 5×10^4 HeLa cells, and $12.5 \mu\text{l}$ cultures ($OD_{620\text{nm}} = 1$) were added in. Based on the number of rounding cells in the vision field, rough ratios of rounding cells were calculated.

(Fig. 3(b)) at 3-h past infection (hpi), indicating that SMG reduced the cytotoxicity of *Y. pestis* to some extent.

The xCELLigence RTCA system could be used to quantitatively assess the degree of cytotoxicity (Roshan Moniri *et al.*, 2015). Due to differences in cell growth in the first 12 h (Fig. 4(a)), the cell index was normalized at the 12-h point to eliminate the influence of different cultivated cell number of each well. The cell index data per 2 h from 3-h to 36-h point was reanalysed using GraphPad Prism 5.0 software (Fig. 4(b)). Apoptosis of HeLa cells appeared under SMG condition was relatively less than NG condition, indicating that SMG weakened the cytotoxicity of *Y. pestis*.

Assessment of virulence of *Y. pestis* under SMG

Mice were separately inoculated intraperitoneally with *Y. pestis* grown under SMG or NG conditions. The 40th passage cultures were injected into each mouse with a high (100 CFU) or a low (10 CFU) challenge dose. For the high dose, the actual number of bacteria injected into a mouse was 414

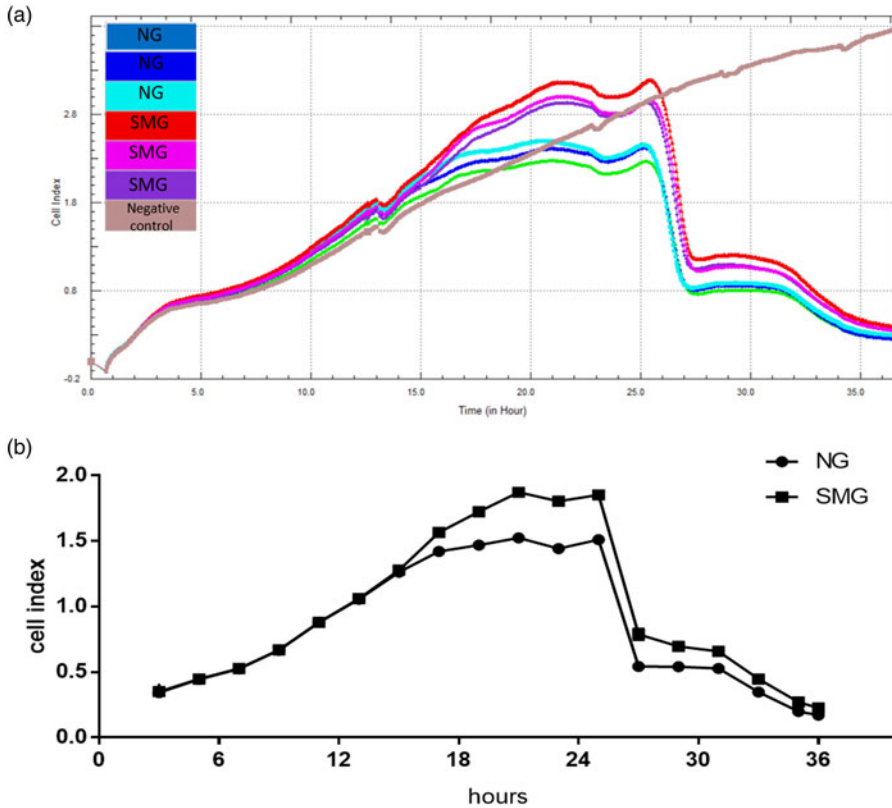


Figure 4. Quantitative Analysis of HeLa cells cytotoxicity by the real-time cell analysis (RTCA). 300 μl of HeLa cell suspension at a concentration of 5×10^5 cells mL^{-1} was added into each well of the E-plate and cultivated in the E-plate for 12 h, and then added 3.75 μl cultures ($OD_{620\text{nm}} = 1.0$) grown under SMG or NG condition into each hole at a MOI of ~ 5 , the cultures grown under SMG and NG conditions were respectively into each well in triplicate. (a) The last well containing HeLa cells only was regarded as the negative control. (b) After being normalized by index data at 12 h, the cell index data was drawn per 2 h during the period of 3 to 36 h using GraphPad Prism 5.0 software.

CFU for the SMG group and 323 CFU for the NG group. For the low dose, the actual number of bacteria was 42 CFU for SMG and 36 CFU for NG.

At the higher challenge dose, 7 of 8 mice infected with the SMG-grown *Y. pestis* survived on the day 3 post infection (p.i.), while 4 of 8 mice with NG group died despite starting with relatively low numbers of inoculated bacteria. Upon day 5 p.i., all mice infected with NG-grown *Y. pestis* died while the deaths of all mice with SMG were delayed by 3 days (Fig. 5(a)). A similar tendency was also seen at the lower challenge dose as shown in Fig. 5(b). The difference of survival percentage between the two groups of infected mice was statistically significant ($p = 0.0006$). This result indicated that the virulence of *Y. pestis* was weakened under a microgravity environment.

Detection of the differential expressions of 218 genes between SMG and NG groups

To identify the differential expressions of genes which were regulated by SMG condition relative to NG condition, RNA-seq and quantitative RT-PCR technologies were used to compare the transcripts between SMG and NG groups (The raw data of RNA-seq was submitted to the SRA database on NCBI Accession to cite for these SRA data: PRJNA700490). According to the RNA-seq data, a

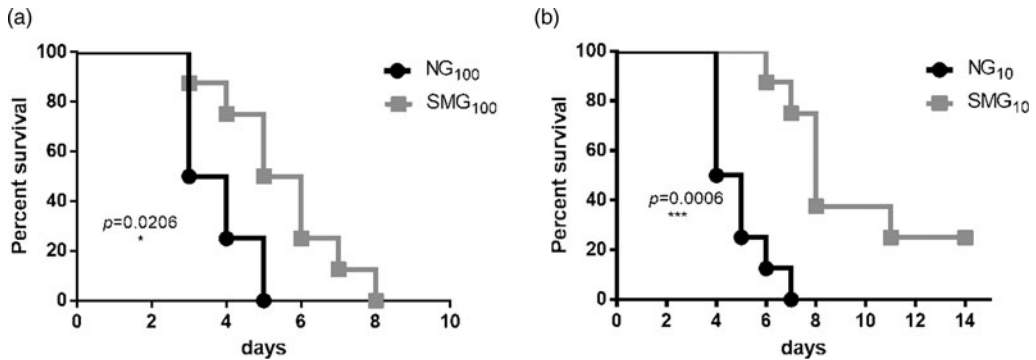


Figure 5. Survival curves of BABL/c mice infected by *Y. pestis* grown under SMG and NG conditions. (a) Each mouse was intraperitoneally inoculated by actual dose of 414 CFU of SMG group and 323 CFU of NG group. The survival curve had statistical significance ($p = 0.0206$). (b) Mice were challenged with 42 CFU of SMG cultures and 36 CFU of NG cultures. The survival curve indicated a significant difference between two groups ($p = 0.0006$). Survival was monitored for 14 days.

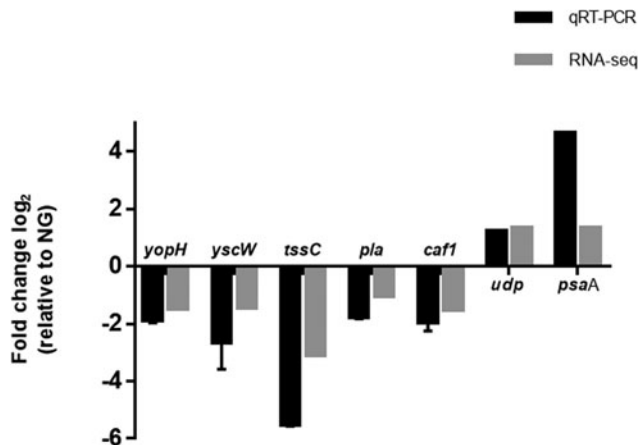


Figure 6. Relative expression of SMG group relative to NG group by qRT-PCR (black) and RNA-seq (grey).

total of 218 genes were found, including 91 upregulated and 127 downregulated genes which were indicated by at least a 2-fold change in expression (with 95% confidence) in the SMG group relative to the NG group. According to the KEGG pathway database, some of the differentially regulated genes were classified into 32 functional classes (Table 3), of them most were related to biosynthesis and material metabolism. We also found different expression of some virulence-related genes, such as YP_RS21365 (*yopE*), YP_RS21080 (*yopH*) in *Yersinia* infection pathway and YP_RS19170 (*virG/yscW*) in the bacterial secretion system pathway (Table 4).

Of all the differentially expressed genes, we noticed that dozens of well-characterized virulence genes of *Y. pestis* were downregulated, including genes responsible for Type-III secretion system (*yopH*, *yopE*, *yscW*, *yscA*, *yscB*, *lcrH*), for iron metabolism (*fyuA*, *irp* and *ybt* cluster), *cafI* operon encoding capsular antigen and the *pla* gene encoding plasminogen-activating protease. The downregulation of these genes might partially account for the impaired virulence observed in cell cytotoxicity and mice infection assays. The RT-PCR result correlated well with the RNA-seq data as shown in Fig. 6, although the relative values were obtained higher based on RT-PCR than that on RNA-seq.

Table 1. Primers of the target genes used in qRT-PCR

Gene name	Primers (forward / reverse, 5'-3')
<i>psaA</i>	ACTGTCAAGCAGGGAAACAC/ ACCAACATAGTCACCATCGG
<i>udp</i>	ACCTTCTACCTCCATTGCCG/ TGAATAGCCCTGTTGTCCC
<i>tssC</i>	ATATGGGCAGTTTGGTG GGG/ ATGCTTGGGGAAGAAGAGGT
<i>yopH</i>	AATCTCTGTTTCCTGTGGTTC/ TATTGCGTTTTGTTTCTGCT
<i>yscW</i>	TGGGTTGTATGAGGGGAAAG/TAAGCTTTTGCTGAGCCACCGCCTG
<i>cafI</i>	CCTAAGGTAAACGGTGAGAA/ ATTGAGCGAACAAGAAATC
<i>pla</i>	CTTTATGACGCAGAAACAGG/ AAATGAGTATGGATCCCAGG
16s rRNA	GAGCGGCGGACGGGTGAGTA/GGGCACATCTGATGGCATGA

Table 2. The reaction system of qPCR

Components	Volume (20 μ l)
cDNA	2 μ l
SYBR® Green I Master	10 μ l
forward primer	0.8 μ l
reverse primer	0.8 μ l
RNase-free Water	6.4 μ l

Table 3. The reaction procedure of qPCR

Procedure	Cycles	Temperature ($^{\circ}$ C)	Time
Pre-incubation	1	95	5 min
Amplification	55	95	15 s
		56	10 s
		72	15 s
		95	5 s
Melting curve	1	65	1 min
		97	0 s
		40	30 s

Discussion

In recent years, microgravity-induced responses of many pathogenic bacteria have been widely characterized. *Salmonella typhimurium* grown under SMG exhibited increased virulence and resistance to acid stress and macrophage killing (Nickerson *et al.*, 2000; Wilson *et al.*, 2002b), while diminished virulence was found in *Staphylococcus aureus* grown under SMG (Castro *et al.*, 2011). In our study, *Y. pestis* showed increased biofilm formation ability and reduced cytotoxicity and virulence under SMG. These results suggest different microbes respond differently to the microgravity. The research scope in this field has been extended beyond pathogens directly related to spaceflight (Klaus and Howard, 2006; Singh *et al.*, 2018). Phenotypic variation accelerated by stimulated microgravity or spaceflight broadens our insights into virulence mechanisms of various bacteria. In this study, SMG-induced changes of both pathogenesis and biofilm formation were observed in *Y. pestis* strain 201 grown for 40 successive passages within the HARV bioreactor. In agreement with the research finding of Rosenzweig's group

Table 4. KEGG pathway of differentially regulated genes in *Y. pestis* under SMG condition

NO	Pathways	Upregulated genes		Downregulated genes	
		NO.	Gene ID	NO.	Gene ID
1	Sulfur metabolism	0		7	YP_RS17660/YP_RS00945 (<i>tauB</i>)/YP_RS20425 (<i>ssuE</i>)/YP_RS00955 (<i>tauD</i>)/YP_RS13710/ YP_RS00940(<i>tauA</i>)/ YP_RS00950(<i>tauC</i>)
2	Yersinia infection	0		3	YP_RS21365(<i>yopE</i>)/ YP_RS21080(<i>yopH</i>)/ YP_RS21315
3	ABC transporters	5	YP_RS07290(<i>mgIB</i>)/ YP_RS07295(<i>mgIA</i>)/ YP_RS07300(<i>mgIC</i>)/ YP_RS06540(<i>artJ</i>)/ YP_RS17015(<i>ugpA</i>)	12	YP_RS12700(<i>proV</i>)/ YP_RS12690(<i>proX</i>)/ YP_RS12695(<i>proW</i>)/ YP_RS10305(<i>oppC</i>)/ YP_RS18560/ YP_RS00945(<i>tauB</i>)/ YP_RS01915/ YP_RS13870/ YP_RS13710/ YP_RS00940(<i>tauA</i>)/ YP_RS06645/ YP_RS00950 (<i>tauC</i>)
4	Glycerophospholipid metabolism	4	YP_RS17260(<i>glpD</i>)/ YP_RS16860(<i>glpC</i>)/ YP_RS16850(<i>glpA</i>)/ YP_RS16855(<i>glpB</i>)	0	
5	Galactose metabolism	3	YP_RS05280(<i>galE</i>)/ YP_RS05285(<i>galT</i>)/ YP_RS05290(<i>galK</i>)	0	
6	Bacterial secretion system	2	YP_RS14835(<i>gspS</i>)/ YP_RS20565	5	YP_RS19195/YP_RS19170 (<i>vgrG</i>)/YP_RS19175 (<i>tssH</i>)/YP_RS19145(<i>tssJ</i>)/ YP_RS14335
7	Starch and sucrose metabolism	2	YP_RS20055(<i>treC</i>)/ YP_RS20050(<i>treB</i>)	1	YP_RS12855
8	Pyrimidine metabolism	2	YP_RS07315(<i>cdd</i>)/ YP_RS17060(<i>udp</i>)	2	YP_RS10280/YP_RS10810 (<i>yjjG</i>)
9	Amino sugar and nucleotide sugar metabolism	4	YP_RS05280(<i>galE</i>)/ YP_RS05285(<i>galT</i>)/ YP_RS05290(<i>galK</i>)/ YP_RS13745	0	
10	Arginine biosynthesis	2	YP_RS00155(<i>glnA</i>)/ YP_RS03285(<i>argF</i>)	0	
11	beta-Lactam resistance	0		2	YP_RS04730 /YP_RS10305 (<i>oppC</i>)

(Continued)

Table 4. (Continued.)

NO	Pathways	Upregulated genes		Downregulated genes	
		NO.	Gene ID	NO.	Gene ID
12	Phosphotransferase system (PTS)	1	YP_RS20050(<i>treB</i>)	1	YP_RS12855
13	Riboflavin metabolism	0		1	YP_RS20425(<i>ssuE</i>)
14	Nitrogen metabolism	1	YP_RS00155(<i>glnA</i>)	0	
15	Purine metabolism	0		4	YP_RS10810(<i>yjjG</i>)/ YP_RS17665/ YP_RS04370(<i>purK</i>)/ YP_RS04375(<i>purE</i>)
16	Glycerolipid metabolism	1	YP_RS00495(<i>glpK</i>)	0	
17	Cationic antimicrobial peptide (CAMP) resistance	0		2	YP_RS01580(<i>degP</i>)/ YP_RS07745
18	Cysteine and methionine metabolism	0		2	YP_RS17660/YP_RS11815
19	Oxidative phosphorylation	1	YP_RS12230(<i>nuoK</i>)	1	YP_RS03960(<i>cyoA</i>)
20	Two-component system	3	YP_RS00155(<i>glnA</i>)/ YP_RS00150(<i>glnL</i>)/ YP_RS08100	2	YP_RS01580(<i>degP</i>)/ YP_RS04730
21	O-Antigen nucleotide sugar biosynthesis	1	YP_RS05280(<i>galE</i>)	0	
22	Arginine and proline metabolism	0		1	YP_RS04840
23	Nicotinate and nicotinamide metabolism	0		1	YP_RS10810(<i>yjjG</i>)
24	Quorum sensing	0		3	YP_RS10305(<i>oppC</i>)/ YP_RS18045/ YP_RS11815
25	Glyoxylate and dicarboxylate metabolism	1	YP_RS00155(<i>glnA</i>)	0	
26	Aminoacyl-tRNA biosynthesis	0		1	YP_RS11195(<i>tyrS</i>)
27	Lipopolysaccharide biosynthesis	0		1	YP_RS07745
28	Alanine, aspartate and glutamate metabolism	1	YP_RS00155(<i>glnA</i>)	0	
29	Pentose and glucuronate interconversions	1	YP_RS09105(<i>kduD</i>)	0	
30	Bacterial chemotaxis	1	YP_RS07290(<i>mglB</i>)	0	
31	Flagellar assembly	2	YP_RS08295(<i>flgH</i>)/ YP_RS08100	0	
32	Biosynthesis of amino acids	2	YP_RS00155(<i>glnA</i>)/ YP_RS03285(<i>argF</i>)	1	YP_RS17660

focusing on the short-term effect of SMG on *Y. pestis* cells (Lawal *et al.*, 2010, 2013), the degree of HeLa cells damage was reduced to some extent upon infection of SMG-grown *Y. pestis* compared with NG-grown counterpart. The decreased cytotoxicity could be mainly attributed to repression of type III secretion system (T3SS) function, which allows *Y. pestis* to inject the effector proteins into the cytosol of eukaryotic cells (Cornelis, 2002; Torruellas *et al.*, 2005) and thus impede the phagocytosis and killing from host cells (Rosqvist *et al.*, 1990; Iriarte and Cornelis, 1998). These speculations were also corroborated by our results of RNA-seq data.

The type III secretion system (T3SS) of gram-negative bacteria is responsible for delivering the effector proteins (e.g. Yops, Ysc, and so on) directly into the interior of host cells (Ghosh, 2004). The effector proteins interfere with the host cell's natural immune function, including inhibiting the host's inflammatory response, inhibiting non-specific immune protection, preventing the bacteria from phagocytosis and killing by phagocytes, etc., so that the bacteria can survive and proliferate, and then establish a continuous infection (Torruellas *et al.*, 2005). In addition to the differential expression of the T3SS-related genes, we also observed the changes in the expression of many virulence factors of *Y. pestis* strain 201 such as pH6 antigen (Lindler *et al.*, 1990), Pla (Sebbane *et al.*, 2006; Zimble *et al.*, 2015), F1 antigen (Du *et al.*, 2002) and other iron-metabolism-related proteins (Ybt and FyuA) (Bearden *et al.*, 1997; Fetherston *et al.*, 2010) under SMG condition. The differential expression of these genes might be implicated in virulence attenuation of SMG-grown *Y. pestis*. However, this alteration of virulence phenotype was not observed in mice challenged with 1×10^8 CFU of NG- and SMG-grown *Y. pestis* KIM/D27 by Rosenzweig's group. Similarly, the bacterial cultures of the 20th passage used to infect mice failed to attenuate the virulence (data not shown). In spite of different dose administration and different strain usage between the two studies, we are more inclined to speculate that the long-duration maintenance under SMG might be a more important contributor for the virulence alteration. Then we considered whether the current phenotypic differences were caused by mutations or loss of certain genes, so the *Y. pestis* strain 201, 15th, 35th and 60th bacteria grown under SMG and NG conditions were selected for whole-genome sequencing. The results failed to find obvious single nucleotide polymorphism or fragment insertion-deletion of the target genes, which also shows that the phenotypic change of *Y. pestis* under SMG conditions is not caused by certain gene mutation or fragment insertion-deletion.

Biofilm is a membrane formed by the adhesion of polysaccharides, lipoproteins, fibrin and other substances secreted by bacteria and it can improve the ability of bacteria to adapt to the environment, anti-phagocytosis and drug resistance (Costerton *et al.*, 1999; Mah and O'Toole, 2001; Branda *et al.*, 2005). Enhanced ability of bacterial biofilm formation under SMG condition has been reported in *Salmonella*, *K. pneumoniae* and etc. (Wilson *et al.*, 2002a; Wang *et al.*, 2016). It is generally supposed that the ability of biofilm formation is positively correlated with bacterial pathogenesis. However, the opposite trend of biofilm formation ability and virulence was seen in SMG-grown *Y. pestis*. This phenomenon might be explained by the complex life cycle of *Y. pestis*, in which fleas are used as vectors to involve in bacterial dissemination. *Y. pestis* occurring in natural foci relies on the complex network of dissemination between wild rodents and fleas. *Y. pestis* colonizes the flea guts and gradually forms thick biofilms that block the flea proventriculus. The constant biting of the starving fleas injects the blood containing *Y. pestis* into new host bodies, which promotes the spread of plague (Hinnebusch *et al.*, 2017). We noticed however, that the putative biofilm-related genes of *Y. pestis* didn't exhibit the differential expressions.

Conclusions

In this study, we used HARV to study the phenotypic changes of *Y. pestis* in a microgravity environment. SMG condition reduces the expression of plague-related virulence genes, resulting in weakened virulence, which is different from other Gram-negative bacteria. The blood cells can maintain a continuous suspension state, indicating that bacteria could also face with a microgravity-like environment during the process of disseminating with blood. Therefore, research on pathogens in the microgravity

environment is helpful to study their changes in the body (Lawal *et al.*, 2010). Since the regulation of *Y. pestis* biofilm is a very complicated process, and post-transcriptional regulation is considered to be the most important process (Martínez and Vadyvaloo, 2014), our future work will focus on relevant sRNAs to explore the potential effects on enhanced biofilm formation ability of *Y. pestis* under SMG condition.

Authors contributions

YL performed experiments, analysed the data and wrote the manuscript. LW, YC and YL carried out the experiments and investigated the literature. RY provided overall directions throughout the study. YH designed the experiments, analysed the data, provided overall directions and contributed to manuscript revisions.

Financial support. This study was funded by the Key Program of Logistics Research (Grant No. BWS18J012 & BWS17J030).

Conflict of interest. All authors declare that they have no conflict of interests.

Ethical standards. This study was carried out in compliance with the ARRIVE guidelines. The ethical approval of animals was obtained from the Beijing Institute of Microbiology and Epidemiology Ethics Committee. This article does not contain any studies with human participants performed by any of the authors

Data availability statement. We guarantee that all data in the study are true and reliable. Data to support the findings in this study can be obtained from Ye Li.

References

- Bearden SW, Fetherston JD and Perry RD (1997) Genetic organization of the yersiniabactin biosynthetic region and construction of avirulent mutants in *Yersinia pestis*. *Infection and Immunity* **65**, 1659–1668.
- Branda SS, Vik K, Friedman L and Kolter R (2005) Biofilms: the matrix revisited. *Trends in Microbiology* **13**, 20–26.
- Buchheim JI, Matzel S, Rykova M, Vassilieva G, Ponomarev S, Nichiporuk I, Hörl M, Moser D, Biere K, Feurecker M, Schelling G, Thieme D, Kaufmann I, Thiel M and Choukèr A (2019) Stress related shift toward inflammaging in cosmonauts after long-duration space flight. *Frontiers in Physiology* **10**, 85.
- Castro SL, Nelman-Gonzalez, M, Nickerson CA and Ott CM (2011) Induction of attachment-independent biofilm formation and repression of Hfq expression by low-fluid-shear culture of *Staphylococcus aureus*. *Applied and Environmental Microbiology* **77**, 6368–6378.
- Cetin I and Topcul MR (2019) Evaluation of the cytotoxic effect of Ly2109761 on HeLa cells using the xCELLigence RTCA system. *Oncology Letters* **17**, 683–687.
- Cornelis GR (2002) The *Yersinia* Ysc-Yop ‘type III’ weaponry. *Nature Reviews Molecular Cell Biology* **3**, 742–752.
- Costerton JW, Stewart PS and Greenberg EP (1999) Bacterial biofilms: a common cause of persistent infections. *Science (New York, N.Y.)* **284**, 1318–1322.
- Du Y, Rosqvist R and Forsberg A (2002) Role of fraction 1 antigen of *Yersinia pestis* in inhibition of phagocytosis. *Infection and Immunity* **70**, 1453–1460.
- Fetherston J, Kirillina O, Bobrov AG, Paulley JT and Perry RD (2010) The yersiniabactin transport system is critical for the pathogenesis of bubonic and pneumonic plague. *Infection and Immunity* **78**, 2045–2052.
- Ghosh P (2004) Process of protein transport by the type III secretion system. *Microbiology and Molecular Biology Reviews* **68**, 771–795.
- Hinnebusch BJ, Jarrett CO and Bland DM (2017) “Fleaing” the plague: adaptations of *Yersinia pestis* to its insect vector that lead to transmission. *Annual Review of Microbiology* **71**, 215–232.
- Iriarte M and Cornelis GR (1998) YopT, a new *Yersinia* Yop effector protein, affects the cytoskeleton of host cells. *Molecular Microbiology* **29**, 915–929.
- Klaus DM and Howard HN (2006) Antibiotic efficacy and microbial virulence during space flight. *Trends in Biotechnology* **24**, 131–136.
- Lawal A, Jejelowo OA and Rosenzweig JA (2010) The effects of low-shear mechanical stress on *Yersinia pestis* virulence. *Astrobiology* **10**, 881–888.
- Lawal A, Kirtley ML, van Lier CJ, Erova TE, Kozlova EV, Sha J, Chopra AK and Rosenzweig JA (2013) The effects of modeled microgravity on growth kinetics, antibiotic susceptibility, cold growth, and the virulence potential of a *Yersinia pestis* ymoA-deficient mutant and its isogenic parental strain. *Astrobiology* **13**, 821–832.
- Lindler LE, Klempner MS and Straley SC (1990) *Yersinia pestis* pH 6 antigen: genetic, biochemical, and virulence characterization of a protein involved in the pathogenesis of bubonic plague. *Infection and Immunity* **58**, 2569–2577.
- Mah T-FC and O’Toole GA (2001) Mechanisms of biofilm resistance to antimicrobial agents. *Trends in Microbiology* **9**, 34–39.

- Martínez L and Vadyvaloo V (2014) Mechanisms of post-transcriptional gene regulation in bacterial biofilms. *Frontiers in cellular and infection microbiology* **4**, 38.
- Moniri MR, Young A, Reinheimer K, Rayat J and Warnock GL (2015) Dynamic assessment of cell viability, proliferation and migration using real time cell analyzer system (RTCA). *Cytotechnology* **67**, 379–386.
- Nickerson CA, Ott CM, Mister SJ, Morrow BJ, Burns-Keliher L and Pierson DL (2000) Microgravity as a novel environmental signal affecting *Salmonella enterica* serovar Typhimurium virulence. *Infection and Immunity* **68**, 3147–3152.
- Nickerson CA, Ott CM, Wilson JW, Ramamurthy R and Pierson DL (2004) Microbial responses to microgravity and other low-shear environments. *Microbiology and Molecular Biology Reviews* **68**, 345–361.
- Pan T, Khare S, Ackah F, Huang B, Zhang W, Gabos S, Jin C and Stampfl M (2013) In vitro cytotoxicity assessment based on KC (50) with real-time cell analyzer (RTCA) assay. *Computational Biology and Chemistry* **47**, 113–120.
- Perry R and Fetherston JD (1997) *Yersinia pestis*—etiologic agent of plague. *Clinical Microbiology Reviews* **10**, 35–66.
- Pujol C and Bliska JB (2005) Turning *Yersinia* pathogenesis outside in: subversion of macrophage function by intracellular yersiniae. *Clinical Immunology* **114**, 216–226.
- Qiao L, Xu Z, Zhao T, Zhao Z, Shi M, Zhao RC, Ye L and Zhang X (2008) Suppression of tumorigenesis by human mesenchymal stem cells in a hepatoma model. *Cell Research* **18**, 500–507.
- Rosenzweig J, Abogunde O, Thomas K, Lawal A, Nguyen YU and Jejelowo SO (2010) Spaceflight and modeled microgravity effects on microbial growth and virulence. *Applied Microbiology and Biotechnology* **85**, 885–891.
- Rosqvist R, Forsberg A, Rimpiläinen M, Bergman T and Wolf-Watz H (1990) The cytotoxic protein YopE of *Yersinia* obstructs the primary host defence. *Molecular Microbiology* **4**, 657–667.
- Sebbane F, Jarrett CO, Gardner D, Long D and Hinnebusch BJ (2006) Role of the *Yersinia pestis* plasminogen activator in the incidence of distinct septicemic and bubonic forms of flea-borne plague. *Proceedings of the National Academy of Sciences of the United States of America* **103**, 5526–5530.
- Singh NK, Wood JM, Karouia F and Venkateswaran K (2018) Succession and persistence of microbial communities and antimicrobial resistance genes associated with international space station environmental surfaces. *Microbiome* **6**, 204.
- Song Y, Tong Z, Wang J, Wang L, Guo Z, Han Y, Zhang J, Pei D, Zhou D, Qin H, Pang X, Han Y, Zhai J, Li M, Cui B, Qi Z, Jin L, Dai R, Chen F, Li S, Ye C, Du Z, Lin W, Wang J, Yu J, Yang H, Wang J, Huang P and Yang R (2004) Complete genome sequence of *Yersinia pestis* strain 91001, an isolate avirulent to humans. *DNA Research* **11**, 179–197.
- Sonnenfeld G and Shearer WJN (2002) Immune function during space flight. *Nutrition (Burbank, Los Angeles County, Calif.)* **18**, 899–903.
- Toruellas J, Jackson MW, Pennock JW and Plano GV (2005) The *Yersinia pestis* type III secretion needle plays a role in the regulation of Yop secretion. *Molecular Microbiology* **57**, 1719–1733.
- Wang H, Yan Y, Rong D, Wang J, Wang H, Liu Z, Wang J, Yang R and Han Y (2016) Increased biofilm formation ability in *Klebsiella pneumoniae* after short-term exposure to a simulated microgravity environment. *MicrobiologyOpen* **5**, 793–801.
- Wilson JW, Ott CM, Ramamurthy R, Porwollik S, McClelland M, Pierson DL and Nickerson CA (2002a) Low-Shear modeled microgravity alters the *Salmonella enterica* serovar typhimurium stress response in an RpoS-independent manner. *Applied and Environmental Microbiology* **68**, 5408–5416.
- Wilson JW, Ramamurthy R, Porwollik S, McClelland M, Hammond T, Allen P, Ott CM, Pierson DL and Nickerson CA (2002b) Microarray analysis identifies *Salmonella* genes belonging to the low-shear modeled microgravity regulon. *Proceedings of the National Academy of Sciences of the United States of America* **99**, 13807–13812.
- Wilson JW, Ott CM, Hoener zu Bentrup K, Ramamurthy R, Quick L, Porwollik S, Cheng P, McClelland M, Tsapraillis G, Radabaugh T, Hunt A, Fernandez D, Richter E, Shah M, Kilcoyne M, Joshi L, Nelman-Gonzalez M, Hing S, Parra M and Dumars P (2007) Space flight alters bacterial gene expression and virulence and reveals a role for global regulator Hfq. *Proceedings of the National Academy of Sciences of the United States of America* **104**, 16299–16304.
- Zimble DL, Schroeder JA, Eddy JL, Latham WW (2015) Early emergence of *Yersinia pestis* as a severe respiratory pathogen. *Nature Communications* **6**, 7487.